

A semi-Lagrangian deterministic solver for a hybrid quantum-classical nanoMOSFET

Naoufel Ben Abdallah, José Antonio Carrillo, Francesco Vecil

MOMINE, 14-21/06/2008

Outline

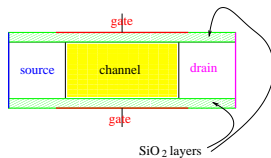
- 1 The model
 - Geometry
 - Mathematical model
- 2 Numerical methods for the Schrödinger-Poisson block
 - Newton schemes
 - Solvers for Schrödinger and Poisson
- 3 Solvers for the BTE block
 - BTE discretizations
 - Linear advection
 - PWENO interpolations
- 4 Experiments
 - Equilibria
 - Time-dependent simulations

Outline

- 1 The model
 - Geometry
 - Mathematical model
- 2 Numerical methods for the Schrödinger-Poisson block
 - Newton schemes
 - Solvers for Schrödinger and Poisson
- 3 Solvers for the BTE block
 - BTE discretizations
 - Linear advection
 - PWENO interpolations
- 4 Experiments
 - Equilibria
 - Time-dependent simulations

The model

We afford the simulation of a nanoscaled MOSFET.



Dimensional coupling

x -dimension is longer than z -dimension, therefore we adopt a different description:

- along x -dimension electrons behave like **particles**, their movement being described by the Boltzmann Transport Equation;
- along z -dimension electrons confined in a potential well behave like **waves**, moreover they are supposed to be at equilibrium, therefore their state is given by the stationary-state Schrödinger equation.

The model

Subband decomposition

Electrons in different energy levels, also called *sub-bands*, another name for the **eigenvalues of the Schrödinger equation**, have to be considered independent populations, so that we have to transport them for separate.

Coupling between dimensions

Dimensions and subbands are coupled in the Poisson equation for the computation of the electrostatic field in the expression of the total density.

Coupling between subbands

Subbands are also coupled in the scattering operator, where the carriers are allowed to jump from an energy level to another one.

The model

Subband decomposition

Electrons in different energy levels, also called *sub-bands*, another name for the **eigenvalues of the Schrödinger equation**, have to be considered independent populations, so that we have to transport them for separate.

Coupling between dimensions

Dimensions and subbands are coupled in the Poisson equation for the computation of the electrostatic field in the expression of the total density.

Coupling between subbands

Subbands are also coupled in the scattering operator, where the carriers are allowed to jump from an energy level to another one.

The model

Subband decomposition

Electrons in different energy levels, also called *sub-bands*, another name for the **eigenvalues of the Schrödinger equation**, have to be considered independent populations, so that we have to transport them for separate.

Coupling between dimensions

Dimensions and subbands are coupled in the Poisson equation for the computation of the electrostatic field in the expression of the total density.

Coupling between subbands

Subbands are also coupled in the scattering operator, where the carriers are allowed to jump from an energy level to another one.

Outline

- 1 **The model**
 - Geometry
 - **Mathematical model**
- 2 Numerical methods for the Schrödinger-Poisson block
 - Newton schemes
 - Solvers for Schrödinger and Poisson
- 3 Solvers for the BTE block
 - BTE discretizations
 - Linear advection
 - PWENO interpolations
- 4 Experiments
 - Equilibria
 - Time-dependent simulations

The model

BTE

The Boltzmann Transport Equation (one for each band) reads

$$\frac{\partial f_p}{\partial t} + \frac{1}{\hbar} \nabla_k \epsilon_p^{\text{kin}} \cdot \nabla_x f_p - \frac{1}{\hbar} \nabla_x \epsilon_p^{\text{pot}} \cdot \nabla_k f_p = \mathcal{Q}_p[f], \quad f_p(t=0, x, k) = \rho_p^{\text{eq}}(x) M(k).$$

Schrödinger-Poisson block

$$-\frac{\hbar^2}{2} \frac{d}{dz} \left[\frac{1}{m_*} \frac{d\chi_p[V]}{dz} \right] - q(V + V_c) \chi_p[V] = \epsilon_p^{\text{pot}}[V] \chi_p[V]$$

$\{\chi_p\}_p \subseteq H_o^1(0, l_z)$ orthonormal basis

$$-\text{div} [\epsilon_R \nabla V] = -\frac{q}{\epsilon_0} \left(\sum_p \rho_p |\chi_p[V]|^2 - N_D \right)$$

plus boundary conditions.

These two equations cannot be decoupled because we need the **eigenfunctions** to compute the potential (in the expression of the **total density**), and we need the potential to compute the eigenfunctions.

The model

BTE

The Boltzmann Transport Equation (one for each band) reads

$$\frac{\partial f_p}{\partial t} + \frac{1}{\hbar} \nabla_k \epsilon_p^{kin} \cdot \nabla_x f_p - \frac{1}{\hbar} \nabla_x \epsilon_p^{pot} \cdot \nabla_k f_p = \mathcal{Q}_p[f], \quad f_p(t=0, x, k) = \rho_p^{eq}(x) M(k).$$

Schrödinger-Poisson block

$$-\frac{\hbar^2}{2} \frac{d}{dz} \left[\frac{1}{m_*} \frac{d\chi_p[V]}{dz} \right] - q(V + V_c) \chi_p[V] = \epsilon_p^{pot}[V] \chi_p[V]$$

$\{\chi_p\}_p \subseteq H_o^1(0, l_z)$ orthonormal basis

$$-\text{div} [\epsilon_R \nabla V] = -\frac{q}{\epsilon_0} \left(\sum_p \rho_p |\chi_p[V]|^2 - N_D \right)$$

plus boundary conditions.

These two equations cannot be decoupled because we need the **eigenfunctions** to compute the potential (in the expression of the **total density**), and we need the potential to compute the eigenfunctions.

The model

The collision operator

The collision operator takes into account the electron-optical phonon scattering mechanism. It reads

$$\mathcal{Q}_p[f] = \sum_{p'} \int_{\mathbb{R}^2} [S_{(p',k') \rightarrow (p,k)} f_{p'}(k') - S_{(p,k) \rightarrow (p',k')} f_p(k)] dk',$$

with

$$S_{(p,k) \rightarrow (p',k')} = S_{(p,k) \rightarrow (p',k')}^+ + S_{(p,k) \rightarrow (p',k')}^-$$

$$S_{(p,k) \rightarrow (p',k')}^+ = (N+1)C \frac{1}{W_{p,p'}} \delta(\epsilon' - \epsilon - \hbar\omega)$$

$$S_{(p,k) \rightarrow (p',k')}^- = NC \frac{1}{W_{p,p'}} \delta(\epsilon' - \epsilon + \hbar\omega)$$

Meaning of the parameters

Bose-Einstein distribution

$$N = \frac{1}{e^{\frac{\hbar\omega}{k_B T_L}} - 1}$$

is the number of phonons with frequency ω assuming Bose-Einstein distribution.

Effective distance (overlapping integral)

$$\frac{1}{W_{p,p'}} = \int_0^{L_z} |\chi_p|^2 |\chi_{p'}|^2 dz$$

is an effective distance over which particles in sub-bands p and p' interact.

Total energy

$$\epsilon = \epsilon_p^{pot}(x) + \epsilon^{kin}(k)$$

is the energy of an electron in sub-band p .

Meaning of the parameters

Bose-Einstein distribution

$$N = \frac{1}{e^{\frac{\hbar\omega}{k_B T_L}} - 1}$$

is the number of phonons with frequency ω assuming Bose-Einstein distribution.

Effective distance (overlapping integral)

$$\frac{1}{W_{p,p'}} = \int_0^{L_z} |\chi_p|^2 |\chi_{p'}|^2 dz$$

is an effective distance over which particles in sub-bands p and p' interact.

Total energy

$$\epsilon = \epsilon_p^{pot}(x) + \epsilon^{kin}(k)$$

is the energy of an electron in sub-band p .

Meaning of the parameters

Bose-Einstein distribution

$$N = \frac{1}{e^{\frac{\hbar\omega}{k_B T_L}} - 1}$$

is the number of phonons with frequency ω assuming Bose-Einstein distribution.

Effective distance (overlapping integral)

$$\frac{1}{W_{p,p'}} = \int_0^{L_z} |\chi_p|^2 |\chi_{p'}|^2 dz$$

is an effective distance over which particles in sub-bands p and p' interact.

Total energy

$$\epsilon = \epsilon_p^{pot}(x) + \epsilon^{kin}(k)$$

is the energy of an electron in sub-band p .

The model

Band structure

The band structure is taken in the parabolic-band approximation:

$$\epsilon^{kin}(k) = \frac{\hbar^2 |k|^2}{2m_*}.$$

Outline

- 1 The model
 - Geometry
 - Mathematical model
- 2 Numerical methods for the Schrödinger-Poisson block
 - Newton schemes
 - Solvers for Schrödinger and Poisson
- 3 Solvers for the BTE block
 - BTE discretizations
 - Linear advection
 - PWENO interpolations
- 4 Experiments
 - Equilibria
 - Time-dependent simulations

The Newton scheme

The functional

Solving the Schrödinger-Poisson block

$$-\frac{\hbar^2}{2} \frac{d}{dz} \left[\frac{1}{m_*} \frac{d\chi_p[V]}{dz} \right] - q(V + V_c) \chi_p[V] = \epsilon_p^{pot}[V] \chi_p[V]$$

$$-\text{div} [\epsilon_R \nabla V] = -\frac{q}{\epsilon_0} \left(\sum_p \rho_p |\chi_p[V]|^2 - N_D \right)$$

is equivalent to minimizing, under the constraints of the Schrödinger equation, the functional $P[V]$

$$P[V] = -\text{div} (\epsilon_R \nabla V) + \frac{q}{\epsilon_0} \left(\sum_p \rho_p |\chi_p[V]|^2 - N_D \right),$$

The scheme

which is achieved by means of a Newton scheme

$$dP(V^{old}, V^{new} - V^{old}) = -P[V^{old}].$$

The Newton scheme

The functional

Solving the Schrödinger-Poisson block

$$-\frac{\hbar^2}{2} \frac{d}{dz} \left[\frac{1}{m_*} \frac{d\chi_p[V]}{dz} \right] - q(V + V_c) \chi_p[V] = \epsilon_p^{pot}[V] \chi_p[V]$$

$$-\text{div} [\epsilon_R \nabla V] = -\frac{q}{\epsilon_0} \left(\sum_p \rho_p |\chi_p[V]|^2 - N_D \right)$$

is equivalent to minimizing, under the constraints of the Schrödinger equation, the functional $P[V]$

$$P[V] = -\text{div} (\epsilon_R \nabla V) + \frac{q}{\epsilon_0} \left(\sum_p \rho_p |\chi_p[V]|^2 - N_D \right),$$

The scheme

which is achieved by means of a Newton scheme

$$dP(V^{old}, V^{new} - V^{old}) = -P[V^{old}].$$

The iterations

Derivatives

The Gâteaux-derivatives of the eigenproperties are needed:

$$d\epsilon_p(V, U) = -q \int U(\zeta) |\chi_p[V](\zeta)|^2 d\zeta$$

$$d\chi_p(V, U) = -q \sum_{p' \neq p} \frac{\int U(\zeta) \chi_p[V](\zeta) \chi_{p'}[V](\zeta) d\zeta}{\epsilon_p[V] - \epsilon_{p'}[V]} \chi_{p'}[V](z).$$

Iterations

After computing the Gâteaux-derivative of the density and developing calculations, we are led to a Poisson-like equation

$$-\operatorname{div}(\epsilon_R \nabla V^{new}) + \int_0^{l_z} \mathcal{A}[V^{old}](z, \zeta) V^{new}(\zeta) d\zeta$$

$$= -\frac{q}{\epsilon_0} \left(\sum_p \rho_p |\chi_p[V^{old}]|^2 - N_D \right) + \int_0^{l_z} \mathcal{A}[V^{old}](z, \zeta) V^{old}(\zeta) d\zeta,$$

where $\mathcal{A}[V]$ is essentially the Gâteaux-derivative of the functional $P[V]$.

The iterations

Derivatives

The Gâteaux-derivatives of the eigenproperties are needed:

$$d\epsilon_p(V, U) = -q \int U(\zeta) |\chi_p[V](\zeta)|^2 d\zeta$$

$$d\chi_p(V, U) = -q \sum_{p' \neq p} \frac{\int U(\zeta) \chi_p[V](\zeta) \chi_{p'}[V](\zeta) d\zeta}{\epsilon_p[V] - \epsilon_{p'}[V]} \chi_{p'}[V](z).$$

Iterations

After computing the Gâteaux-derivative of the density and developing calculations, we are led to a Poisson-like equation

$$-\operatorname{div}(\epsilon_R \nabla V^{new}) + \int_0^{l_z} \mathcal{A}[V^{old}](z, \zeta) V^{new}(\zeta) d\zeta$$

$$= -\frac{q}{\epsilon_0} \left(\sum_p \rho_p |\chi_p[V^{old}]|^2 - N_D \right) + \int_0^{l_z} \mathcal{A}[V^{old}](z, \zeta) V^{old}(\zeta) d\zeta,$$

where $\mathcal{A}[V]$ is essentially the Gâteaux-derivative of the functional $P[V]$.

Outline

- 1 The model
 - Geometry
 - Mathematical model
- 2 Numerical methods for the Schrödinger-Poisson block
 - Newton schemes
 - Solvers for Schrödinger and Poisson
- 3 Solvers for the BTE block
 - BTE discretizations
 - Linear advection
 - PWENO interpolations
- 4 Experiments
 - Equilibria
 - Time-dependent simulations

Numerical methods

We need to solve the Schrödinger eigenvalue problem and Poisson equations.

The Schrödinger equation

Equation

$$-\frac{\hbar^2}{2} \frac{d}{dz} \left[\frac{1}{m_*} \frac{d\chi_p}{dz} \right] - q(V + V_c) \chi_p = \epsilon_p \chi_p$$

is discretized by alternate finite differences for the derivatives then the symmetric matrix is diagonalized by a LAPACK routine called DSTEQR.

The Poisson equation

We need to solve equations like

$$-\text{div} [\epsilon_R \nabla V] + \int_0^{t_c} \mathcal{A}(z, \zeta) V(\zeta) d\zeta = \mathcal{B}(z).$$

The derivatives are discretized by finite differences in alternate directions, the integral is computed via trapezoid rule and the linear system is solved by means of a LAPACK routine called DGESV.

Numerical methods

We need to solve the Schrödinger eigenvalue problem and Poisson equations.

The Schrödinger equation

Equation

$$-\frac{\hbar^2}{2} \frac{d}{dz} \left[\frac{1}{m_*} \frac{d\chi_p}{dz} \right] - q(V + V_c) \chi_p = \epsilon_p \chi_p$$

is discretized by alternate finite differences for the derivatives then the symmetric matrix is diagonalized by a LAPACK routine called DSTEQR.

The Poisson equation

We need to solve equations like

$$-\operatorname{div} [\epsilon_R \nabla V] + \int_0^{t_z} \mathcal{A}(z, \zeta) V(\zeta) d\zeta = \mathcal{B}(z).$$

The derivatives are discretized by finite differences in alternate directions, the integral is computed via trapezoid rule and the linear system is solved by means of a LAPACK routine called DGESV.

Numerical methods

We need to solve the Schrödinger eigenvalue problem and Poisson equations.

The Schrödinger equation

Equation

$$-\frac{\hbar^2}{2} \frac{d}{dz} \left[\frac{1}{m_*} \frac{d\chi_p}{dz} \right] - q(V + V_c) \chi_p = \epsilon_p \chi_p$$

is discretized by alternate finite differences for the derivatives then the symmetric matrix is diagonalized by a LAPACK routine called DSTEQR.

The Poisson equation

We need to solve equations like

$$-\text{div} [\epsilon_R \nabla V] + \int_0^{l_z} \mathcal{A}(z, \zeta) V(\zeta) d\zeta = \mathcal{B}(z).$$

The derivatives are discretized by finite differences in alternate directions, the integral is computed via trapezoid rule and the linear system is solved by means of a LAPACK routine called DGESV.

Outline

- 1 The model
 - Geometry
 - Mathematical model
- 2 Numerical methods for the Schrödinger-Poisson block
 - Newton schemes
 - Solvers for Schrödinger and Poisson
- 3 Solvers for the BTE block
 - **BTE discretizations**
 - Linear advection
 - PWENO interpolations
- 4 Experiments
 - Equilibria
 - Time-dependent simulations

Discretization for the transport

Once we have developed the method for updating the band-potential energies, we can focus the attention on solving the transport. Two discretization are proposed.

Runge-Kutta

FDWENO evaluates via dimension-by-dimension approximation the derivatives $\frac{\partial f_p}{\partial x}$ and $\frac{\partial f_p}{\partial k_1}$ and is coupled with the TVD (Total Variation Diminishing) **Runge-Kutta-3** for the time discretization.

Time- & dimensional-splitting

The BTE is split into the solution of the transport and the collisions, then inside the transport we split dimensions and solve linear advection problems:

$$\begin{aligned} \frac{\partial f_p}{\partial t} + \frac{1}{\hbar} \frac{\partial \epsilon^{kin}}{\partial k_1} \frac{\partial f_p}{\partial x} - \frac{1}{\hbar} \frac{\partial \epsilon_p^{pot}}{\partial x} \frac{\partial f_p}{\partial k_1} &= 0 \\ &= Q_p f_p. \end{aligned}$$

Discretization for the transport

Once we have developed the method for updating the band-potential energies, we can focus the attention on solving the transport. Two discretization are proposed.

Runge-Kutta

FDWENO evaluates via dimension-by-dimension approximation the derivatives $\frac{\partial f_p}{\partial x}$ and $\frac{\partial f_p}{\partial k_1}$ and is coupled with the TVD (Total Variation Diminishing) **Runge-Kutta-3** for the time discretization.

Time- & dimensional-splitting

The BTE is split into the solution of the transport and the collisions, then inside the transport we split dimensions and solve linear advection problems:

$$\begin{aligned} \frac{\partial f_p}{\partial t} + \frac{1}{\hbar} \frac{\partial \epsilon^{kin}}{\partial k_1} \frac{\partial f_p}{\partial x} - \frac{1}{\hbar} \frac{\partial \epsilon_p^{pot}}{\partial x} \frac{\partial f_p}{\partial k_1} &= 0 \\ \frac{\partial f_p}{\partial t} &= Q_p f_p. \end{aligned}$$

Discretization for the transport

Once we have developed the method for updating the band-potential energies, we can focus the attention on solving the transport. Two discretization are proposed.

Runge-Kutta

FDWENO evaluates via dimension-by-dimension approximation the derivatives $\frac{\partial f_p}{\partial x}$ and $\frac{\partial f_p}{\partial k_1}$ and is coupled with the TVD (Total Variation Diminishing) **Runge-Kutta-3** for the time discretization.

Time- & dimensional-splitting

The BTE is split into the solution of the transport and the collisions, then inside the transport we split dimensions and solve linear advection problems:

$$\begin{aligned} \frac{\partial f_p}{\partial t} + \frac{1}{\hbar} \frac{\partial \epsilon_p^{kin}}{\partial k_1} \frac{\partial f_p}{\partial x} - \frac{1}{\hbar} \frac{\partial \epsilon_p^{pot}}{\partial x} \frac{\partial f_p}{\partial k_1} &= 0 \\ \frac{\partial f_p}{\partial t} &= Q_p f_p. \end{aligned}$$

Runge-Kutta

The operator

Define the operator

$$L_p(t, f_p) = -\frac{1}{\hbar} \frac{\partial}{\partial k_1} \left[\epsilon^{kin} f_p \right] + \frac{1}{\hbar} \frac{\partial}{\partial x} \left[\epsilon_p^{pot}(t) f_p \right] + \mathcal{Q}_p f_p,$$

Runge-Kutta scheme

then the third order Total Variation Diminishing Runge-Kutta scheme reads

$$\begin{aligned} f_p^{(1)} &= f_p^n + \Delta t L_p(t^n, f_p^n) \\ f_p^{(2)} &= \frac{3}{4} f_p^n + \frac{1}{4} f_p^{(1)} + \frac{1}{4} \Delta t L_p(t^n + \Delta t, f_p^{(1)}) \\ f_p^{n+1} &= \frac{1}{3} f_p^n + \frac{2}{3} f_p^{(2)} + \frac{2}{3} \Delta t L_p \left(t^n + \frac{\Delta t}{2}, f_p^{(2)} \right). \end{aligned}$$

Explicit time-dependence

As a remark, the operator L has an explicit time-dependence, because the drain-source potential drop is applied smoothly.

Runge-Kutta

The operator

Define the operator

$$L_p(t, f_p) = -\frac{1}{\hbar} \frac{\partial}{\partial k_1} [\epsilon^{kin} f_p] + \frac{1}{\hbar} \frac{\partial}{\partial x} [\epsilon_p^{pot}(t) f_p] + \mathcal{Q}_p f_p,$$

Runge-Kutta scheme

then the third order Total Variation Diminishing Runge-Kutta scheme reads

$$\begin{aligned} f_p^{(1)} &= f_p^n + \Delta t L_p(t^n, f_p^n) \\ f_p^{(2)} &= \frac{3}{4} f_p^n + \frac{1}{4} f_p^{(1)} + \frac{1}{4} \Delta t L_p(t^n + \Delta t, f_p^{(1)}) \\ f_p^{n+1} &= \frac{1}{3} f_p^n + \frac{2}{3} f_p^{(2)} + \frac{2}{3} \Delta t L_p\left(t^n + \frac{\Delta t}{2}, f_p^{(2)}\right). \end{aligned}$$

Explicit time-dependence

As a remark, the operator L has an explicit time-dependence, because the drain-source potential drop is applied smoothly.

Runge-Kutta

The operator

Define the operator

$$L_p(t, f_p) = -\frac{1}{\hbar} \frac{\partial}{\partial k_1} \left[\epsilon^{kin} f_p \right] + \frac{1}{\hbar} \frac{\partial}{\partial x} \left[\epsilon_p^{pot}(t) f_p \right] + \mathcal{Q}_p f_p,$$

Runge-Kutta scheme

then the third order Total Variation Diminishing Runge-Kutta scheme reads

$$\begin{aligned} f_p^{(1)} &= f_p^n + \Delta t L_p(t^n, f_p^n) \\ f_p^{(2)} &= \frac{3}{4} f_p^n + \frac{1}{4} f_p^{(1)} + \frac{1}{4} \Delta t L_p(t^n + \Delta t, f_p^{(1)}) \\ f_p^{n+1} &= \frac{1}{3} f_p^n + \frac{2}{3} f_p^{(2)} + \frac{2}{3} \Delta t L_p \left(t^n + \frac{\Delta t}{2}, f_p^{(2)} \right). \end{aligned}$$

Explicit time-dependence

As a remark, the operator L has an explicit time-dependence, because the drain-source potential drop is applied smoothly.

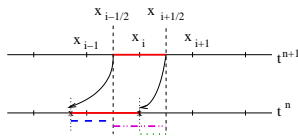
Outline

- 1 The model
 - Geometry
 - Mathematical model
- 2 Numerical methods for the Schrödinger-Poisson block
 - Newton schemes
 - Solvers for Schrödinger and Poisson
- 3 Solvers for the BTE block
 - BTE discretizations
 - **Linear advection**
 - PWENO interpolations
- 4 Experiments
 - Equilibria
 - Time-dependent simulations

Linear advection

Flux Balance Method:

Total mass conservation is forced. It is based on the idea of following backward the characteristics, but integral values are taken instead of point values:



— The averages along the red segments are the same, because we have followed the characteristics backward.

FLUX BALANCE METHOD means evaluating the flux at time t^{n+1} from a balance of fluxes at previous time t^n :

— the average along the purple segment

- - - plus the average along the blue segment

..... minus the average along the green segment

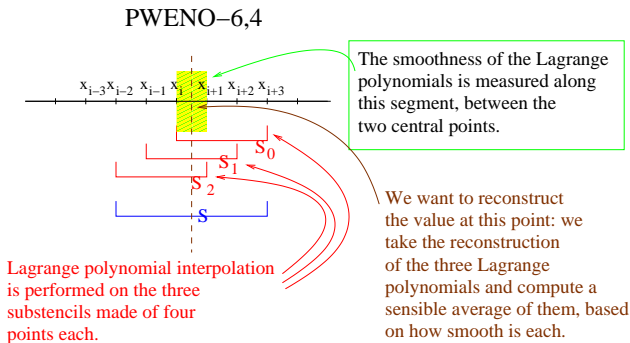
Outline

- 1 The model
 - Geometry
 - Mathematical model
- 2 Numerical methods for the Schrödinger-Poisson block
 - Newton schemes
 - Solvers for Schrödinger and Poisson
- 3 Solvers for the BTE block
 - BTE discretizations
 - Linear advection
 - **PWENO interpolations**
- 4 Experiments
 - Equilibria
 - Time-dependent simulations

Non-oscillatory properties

Essentially Non Oscillatory (ENO) methods are based on on a sensible average of Lagrange polynomial reconstructions.

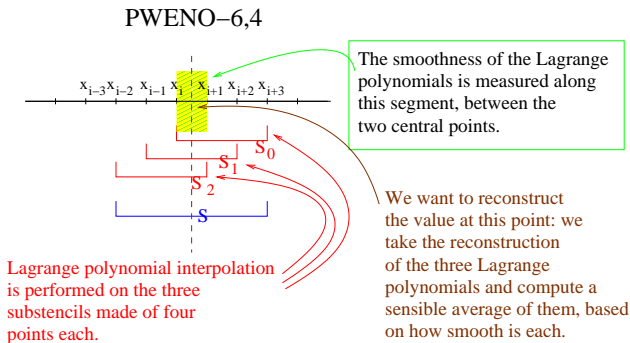
We describe the case of PWENO-6,4: we take a stencil of six points and divide it into three substencils of four points:



Non-oscillatory properties

Essentially Non Oscillatory (ENO) methods are based on on a sensible average of Lagrange polynomial reconstructions.

We describe the case of PWENO-6,4: we take a stencil of six points and divide it into three substencils of four points:



The average

If we note $p_r(x)$ the Lagrange polynomials, PWENO reconstruction reads

$$p_{PWENO}(x) = \omega_0(x)p_0(x) + \omega_1(x)p_1(x) + \omega_2(x)p_2(x).$$

Convex combination.

The convex combination $\{\omega_r(x)\}_r$ must penalize the substencils \mathcal{S}_r in which the $p_r(x)$ have high derivatives.

Smoothness indicators

In order to decide which substencils \mathcal{S}_r are “regular” and which ones are not, we have to introduce the smoothness indicators: we use a weighted sum of the L^2 -norms of the Lagrange polynomials $p_r(x)$ to measure their regularity close to the reconstruction point x . The following smoothness indicators have been proposed by Jiang and Shu:

$$\beta_r = \Delta x \left\| \frac{dp_r}{dx} \right\|_{L^2_{(x_i, x_{i+1})}} + \Delta x^3 \left\| \frac{d^2 p_r}{dx^2} \right\|_{L^2_{(x_i, x_{i+1})}} + \Delta x^5 \left\| \frac{d^3 p_r}{dx^3} \right\|_{L^2_{(x_i, x_{i+1})}}.$$

The average

If we note $p_r(x)$ the Lagrange polynomials, PWENO reconstruction reads

$$p_{PWENO}(x) = \omega_0(x)p_0(x) + \omega_1(x)p_1(x) + \omega_2(x)p_2(x).$$

Convex combination.

The convex combination $\{\omega_r(x)\}_r$ must penalize the substencils \mathcal{S}_r in which the $p_r(x)$ have high derivatives.

Smoothness indicators

In order to decide which substencils \mathcal{S}_r are “regular” and which ones are not, we have to introduce the smoothness indicators: we use a weighted sum of the L^2 -norms of the Lagrange polynomials $p_r(x)$ to measure their regularity close to the reconstruction point x . The following smoothness indicators have been proposed by Jiang and Shu:

$$\beta_r = \Delta x \left\| \frac{dp_r}{dx} \right\|_{L^2_{(x_i, x_{i+1})}} + \Delta x^3 \left\| \frac{d^2 p_r}{dx^2} \right\|_{L^2_{(x_i, x_{i+1})}} + \Delta x^5 \left\| \frac{d^3 p_r}{dx^3} \right\|_{L^2_{(x_i, x_{i+1})}}.$$

The average

If we note $p_r(x)$ the Lagrange polynomials, PWENO reconstruction reads

$$p_{PWENO}(x) = \omega_0(x)p_0(x) + \omega_1(x)p_1(x) + \omega_2(x)p_2(x).$$

Convex combination.

The convex combination $\{\omega_r(x)\}_r$ must penalize the substencils \mathcal{S}_r in which the $p_r(x)$ have high derivatives.

Smoothness indicators

In order to decide which substencils \mathcal{S}_r are “regular” and which ones are not, we have to introduce the smoothness indicators: we use a weighted sum of the L^2 -norms of the Lagrange polynomials $p_r(x)$ to measure their regularity close to the reconstruction point x . The following smoothness indicators have been proposed by Jiang and Shu:

$$\beta_r = \Delta x \left\| \frac{dp_r}{dx} \right\|_{L^2_{(x_i, x_{i+1})}} + \Delta x^3 \left\| \frac{d^2 p_r}{dx^2} \right\|_{L^2_{(x_i, x_{i+1})}} + \Delta x^5 \left\| \frac{d^3 p_r}{dx^3} \right\|_{L^2_{(x_i, x_{i+1})}}.$$

High order reconstruction

Admit for now that the convex combination is given by the normalization

$\omega_r(x) = \frac{\tilde{\omega}_r(x)}{\sum_{s=0}^2 \tilde{\omega}_s(x)}$ of the protoweights $\tilde{\omega}_r(x)$ defined this way:

$$\tilde{\omega}_r(x) = \frac{d_r(x)}{(\epsilon + \beta_r)^2}.$$

Regular reconstruction

Suppose that all the β_r are equal; then we have

$$\omega_r(x) = d_r(x).$$

The optimal order is achieved by Lagrange reconstruction $p_{Lagrange}(x)$ in the whole stencil \mathcal{S} , so if we define $d_r(x)$ to be the polynomials such that

$$p_{Lagrange}(x) = d_0(x)p_0(x) + d_1(x)p_1(x) + d_2(x)p_2(x),$$

then we have achieved the optimal order because $p_{PWENO}(x) = p_{Lagrange}(x)$.

High order reconstruction

Admit for now that the convex combination is given by the normalization

$\omega_r(x) = \frac{\tilde{\omega}_r(x)}{\sum_{s=0}^2 \tilde{\omega}_s(x)}$ of the protoweights $\tilde{\omega}_r(x)$ defined this way:

$$\tilde{\omega}_r(x) = \frac{d_r(x)}{(\epsilon + \beta_r)^2}.$$

Regular reconstruction

Suppose that all the β_r are equal; then we have

$$\omega_r(x) = d_r(x).$$

The optimal order is achieved by Lagrange reconstruction $p_{Lagrange}(x)$ in the whole stencil \mathcal{S} , so if we define $d_r(x)$ to be the polynomials such that

$$p_{Lagrange}(x) = d_0(x)p_0(x) + d_1(x)p_1(x) + d_2(x)p_2(x),$$

then we have achieved the optimal order because $p_{PWENO}(x) = p_{Lagrange}(x)$.

High order reconstruction

Admit for now that the convex combination is given by the normalization

$\omega_r(x) = \frac{\tilde{\omega}_r(x)}{\sum_{s=0}^2 \tilde{\omega}_s(x)}$ of the protoweights $\tilde{\omega}_r(x)$ defined this way:

$$\tilde{\omega}_r(x) = \frac{d_r(x)}{(\epsilon + \beta_r)^2}.$$

High gradients

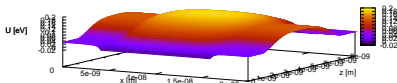
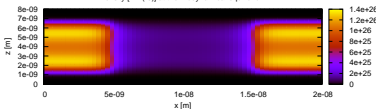
Otherwise, suppose for instance that β_0 is high order than the other ones: in this case S_0 is penalized and most of the reconstruction is carried by the other more “regular” substencils.

Outline

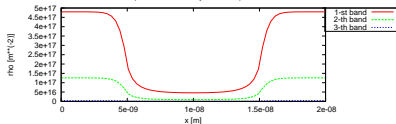
- 1 The model
 - Geometry
 - Mathematical model
- 2 Numerical methods for the Schrödinger-Poisson block
 - Newton schemes
 - Solvers for Schrödinger and Poisson
- 3 Solvers for the BTE block
 - BTE discretizations
 - Linear advection
 - PWENO interpolations
- 4 Experiments
 - **Equilibria**
 - Time-dependent simulations

Thermodynamical equilibrium

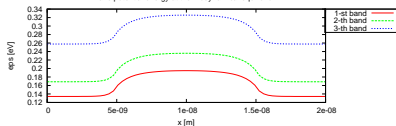
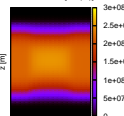
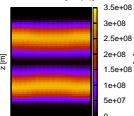
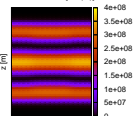
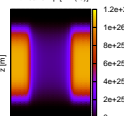
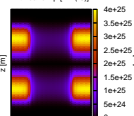
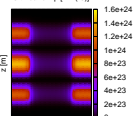
Potential energy at thermodynamical equilibrium

Density [m^{-3}] at thermodynamical equilibrium

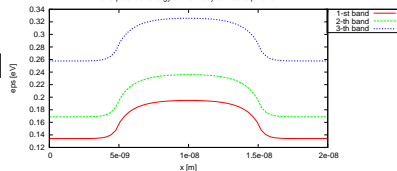
Occupations at thermodynamical equilibrium



Band potential energy at thermodynamical equilibrium

1-th band χ^{*2} [m^{*-1}]2-th band χ^{*2} [m^{*-1}]3-th band χ^{*2} [m^{*-1}]1-th band N_p [m^{*-3}]2-th band N_p [m^{*-3}]3-th band N_p [m^{*-3}]

Band potential energy at thermodynamical equilibrium



Outline

- 1 The model
 - Geometry
 - Mathematical model
- 2 Numerical methods for the Schrödinger-Poisson block
 - Newton schemes
 - Solvers for Schrödinger and Poisson
- 3 Solvers for the BTE block
 - BTE discretizations
 - Linear advection
 - PWENO interpolations
- 4 Experiments
 - Equilibria
 - Time-dependent simulations

Long-time behavior

We propose now some results relative to the long-time behavior of the system.

Plasma oscillations

Close to the ends of the channel, and particularly on the drain side, we observe that the system oscillates around an equilibrium. The frequency has been empirically observed to correspond to the plasma oscillation frequency, given by

$$\omega_{pe} = \sqrt{\frac{N_D q^2}{m_* \epsilon_{Si}}}.$$